

# Measurement of Thermally Induced Warpage of BGA Packages/Substrates Using Phase-Stepping Shadow Moiré

Yinyan Wang and Patrick Hassell  
Electronic Packaging Services, Ltd. Co.  
430 Tenth Street, Suite S002, Atlanta, GA 30318

## ABSTRACT

Phase-stepping technique is applied to the analysis of fringe pattern images of BGAs (Ball Grid Arrays) obtained by shadow moiré. Sensitivity of the fringe pattern analysis is demonstrated to be significantly increased. Thermally induced warpage of BGAs is successfully measured in real-time as the sample is driven through a simulated reflow process. The paper discusses the technique of phase stepping and its application to the shadow moiré method. Applications of the technology are presented.

## Introduction

Complex packaging has led to the widespread use of BGA components in smaller, faster and more condensed applications. Consequently, the range and availability of materials for this type of packaging is also expanding, along with concern over their performance and reliability. The thermomechanical behavior of the BGA substrate, the silicon die, and the encapsulated package is particularly interesting to engineers as adverse behavior, or warpage, can significantly increase rework costs and effect product reliability. The ability to evaluate component package behavior with respect to temperature is important for both interconnect (package to PWB) and performance (internal package stress) purposes.

Common out-of-plane deformations of BGAs are on the order of dozens of micrometers. This amount of deformation is too large for high-sensitivity measuring methods, for example, Twyman-Green interferometry, and too small for general shadow moiré or projection moiré methods. The sensitivity of optical interferometric methods is on the order of one-half wave-length of light. For a 27 mm BGA, if the maximum out-of-plane deformation is 25 $\mu$ m, there will be approximately 80 fringes in the field. Resolving this number of fringes can be very difficult and error prone. Additionally, surface irregularities will cause significant difficulty in extracting information on global deformation. On the other hand, if one uses general shadow moiré method to measure the same out-of-plane deformation, there is only one fringe appearing in the whole field even with a reference grating frequency of 40 lines/mm. With this low level of sensitivity, much of the information used to characterize the surface can be lost. Identifying a method that can bridge the gap between the high-sensitivity methods and the low-sensitivity methods is necessary for the measurement and analysis BGA package/substrate deformation.

## Shadow Moiré

Shadow moiré techniques measures the topography of the surface of a solid object, i.e. its deviation from a planar surface.<sup>1</sup> Fig. 1 illustrates a schematic of shadow moiré technique. Measurements are made by placing a sheet of low expansion quartz glass etched with equally spaced parallel lines parallel to the sample. A beam of white light is then directed onto the glass, and the etched lines on the glass create a shadow on the top surface of the sample. When the sample surface is inclined or curved, a moiré pattern is produced by the geometric interference between the etched lines on the glass and the shadow of those lines on the sample's surface. If the sample is flat and parallel to the grating, there is no warpage and no moiré pattern is produced.

From the governing equation of shadow moiré,

$$w = \frac{Np}{\tan \alpha + \tan \beta} \quad (1)$$

the fringe value (fringe sensitivity) is equal to the pitch ( $p$ ) of the grating if the illumination angle  $\alpha$  is  $45^\circ$  and the observation angle  $\beta$  is  $0^\circ$  as it is sketched in Fig.1. In eq.(1),  $w$  is the out-of-plane displacement and  $N$  is the fringe order. Traditionally, the value of the out-of-plane displacement at an interested point within the field is determined by counting the fringe order at that point. Interpolation is generally necessary because the point does not always fall on a fringe center. The accuracy of the fringe counting method is about 20 percent of a fringe value and the highest sensitivity that shadow moiré can practically reach with this analysis approach is  $25 \mu\text{m}$ .

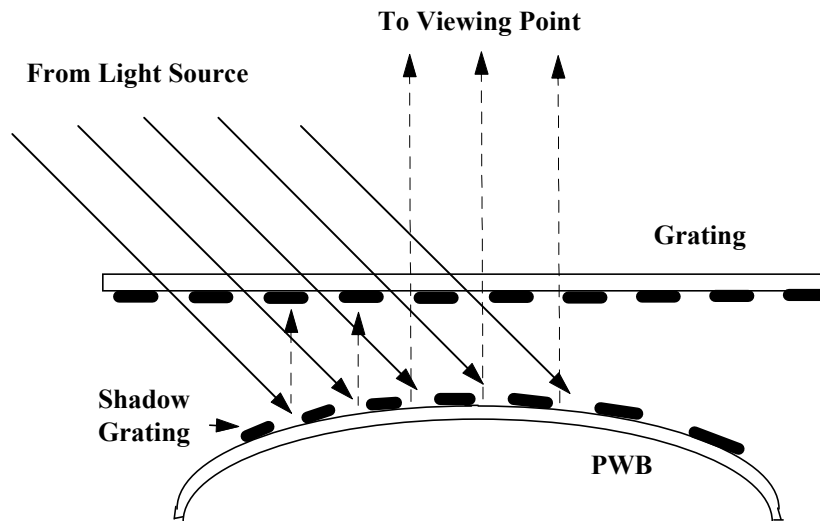


**Fig.1 Schematic of Shadow Moiré.**

## Phase-stepping Technique

It has been demonstrated that shadow moiré fringes are known incremental values of the distance between the sample surface and the grating. When the grating is translated towards or away from the sample surface, the fringes will maintain their fixed distance from the reference grating by moving towards lower order or higher order, respectively. When the grating is translated a distance of  $p$  away from the sample, the fringe will shift up one fringe order. When the grating is translated a distance of fractional  $p$ , the fringe will shift a fractional fringe order. Phase-stepping technique uses multiple fringe patterns that are shifted at a certain amount to obtain fractional fringe orders. The sensitivity of the fringe analysis is increased significantly.

The distribution of light intensity of a fringe pattern obtained from shadow moiré can be approximated by a sinusoidal function <sup>2</sup>,

$$I = I_0 + A \cos[\varphi(x, y)], \quad (2)$$

where,  $I$  is the light intensity,  $I_0$  is the background light,  $A$  is the modulation of the fringe and  $\varphi$  is the phase term. The fringe number  $N$  is simply equal to  $\varphi/2\pi$ , therefore, finding out fringe number  $N$  is to determine phase term  $\varphi$  in eq. (2).

The phase term  $\varphi$  is determined by taking a number of images, shifting the fringe pattern a certain amount for each acquired image, and applying a least squares algorithm to solve for the unknowns of equation (2). <sup>3,4,5</sup> A minimum of three images are necessary because there are three unknowns, background light  $I_0$ , modulation of the fringes  $A$  and phase  $\varphi$ . It is noted that among the three unknowns, only  $\varphi$  is needed to be solved explicitly. Generally, the more images taken, the less error seen due to the system [6]. However, in practice, the fewer images taken, the faster the data acquisition speed and the lower the memory requirement. During in-process measurements of thermally induced warpage, the sample is heated following the temperature profile that simulates the reflow of the manufacturing process. The fringe pattern image needs to be recorded as quickly as possible for a given temperature or time. Three steps of fringe shifting are taken in our application. Considering the three-step technique is more sensitive to step errors, we perform the shifting calibration for the tests [2].

Equation (3) describes the three shifted fringe pattern images. Each pattern is recorded by a CCD camera after the grating is translated one third of one fringe cycle.

$$\begin{aligned} I_1 &= I_0 + A \cos[\varphi(x, y)], \\ I_2 &= I_0 + A \cos\left[\varphi(x, y) - \frac{2\pi}{3}\right], \\ I_3 &= I_0 + A \cos\left[\varphi(x, y) - \frac{4\pi}{3}\right]. \end{aligned}$$

(3)

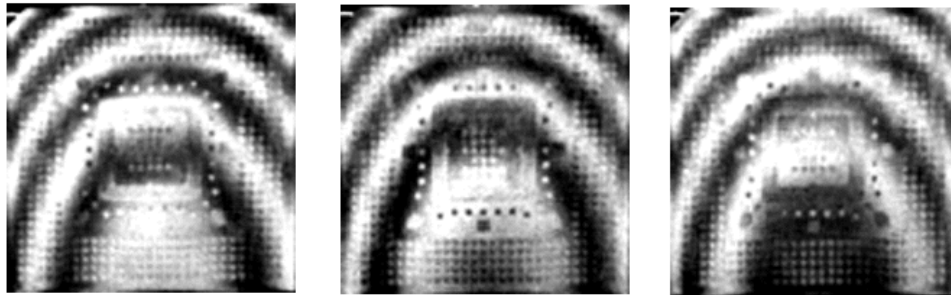
The phase term  $\varphi(x, y)$  is thereby determined,

$$\varphi(x,y) = \arctan \frac{\sqrt{3}(I_2 - I_3)}{(2I_1 - I_2 - I_3)}.$$

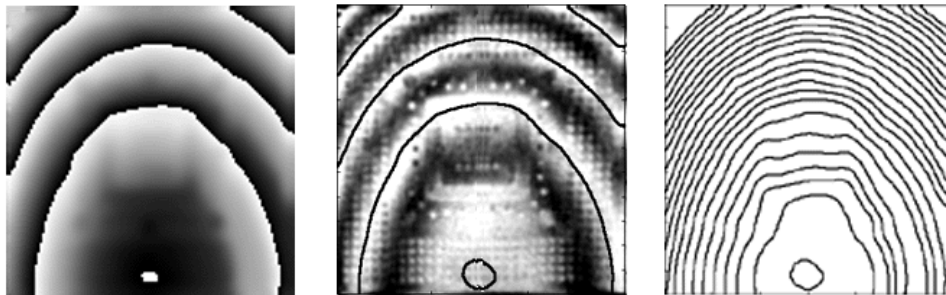
(4)

Due to the nature of arctangent calculation,  $\varphi(x,y)$  can only be determined in the range 0 to  $2\pi$ . The phase ambiguities are removed by an unwrapping process. The average stepping precision is 98% for our system calibration. According to the analyses done by Creath<sup>7</sup>, the resulting error in the data caused by this amount of shifting error for a three-step approach is well within the allowable experimental limit.

Fig.2 shows (a) three phase-stepped fringe pattern images of a BGA laminate substrate, (b) the wrapped phase of the three fringe pattern images, (c) comparison of the contours obtained from the phase-stepping technique and the original fringe pattern, and (d) a contour plot in which the contour interval is 12.7  $\mu\text{m}$ . From the resulting data matrix of the calculation, a contour map can be plotted with a designated contour interval. When the contour interval is set at the level of the fringe sensitivity, the plotted contour lines should fall onto the center of the fringe lines if the phase calculation is accurate (see Fig.2 (c)). The fine features of the sample surface are revealed by the contour plot with fine intervals in Fig.2 (d). Fine features cannot be observed if traditional fringe counting methodology is used to analyze the fringe data.



**(a) Three Shifted Fringe Images of a BGA.**



**(b) Wrapped Phase Image**

**(c) Comparison of the Contour Map with the Fringe Pattern.**

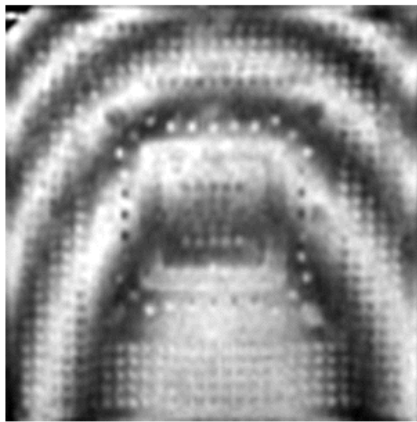
**(d) Contour Map with an Interval of 12.7 Micrometers.**

**Fig.2 Fringe Patterns That are Used and Obtained in Phase Stepping Technique and the Resulting Contours.**

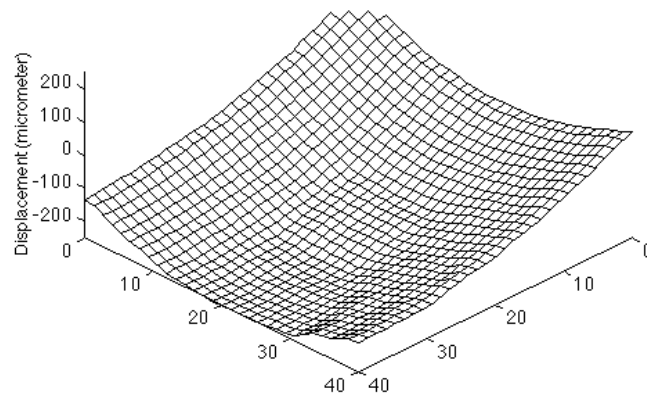
Phase-shifting technique does *not* increase the sensitivity of the measurement method. It increases the sensitivity of fringe pattern image recognition.<sup>1</sup> It makes use of the gray level information contained in the fringe pattern images so that it resolves the fractional fringe order. Since the technique divides the gray level of the light intensity of a fringe image into 256 degrees, it can, theoretically speaking, resolve the fractional fringe to 1/256. In practice, a resolution of 0.01 fringe order is widely accepted.<sup>1,8,9,11</sup>

One important advantage of phase-stepping is that the direction of the warpage is automatically determined due to the nature of the fringe shifting. During the 3 step process, fringes converge or diverge accordingly as the grating is raised or lowered. The ability to automatically determine fringe order not only eliminates a primary source of analysis error, but it also allows for the automated generation of the displacement field matrix across the entire observed area.

The fringe pattern image obtained by shadow moiré provides the contour map of the distances between the sample surface and the plane of the reference grating. Although the initial fringe pattern image depends upon the alignment of the sample with respect to the reference grating, the measurement of the warpage of the sample is not affected by any rigid body rotation or translation of the sample. The rigid body movements of the sample can be easily eliminated when the resulting displacement is normalized to a reference plane. In our applications, two position normalization techniques are available. First, the warped substrate is rotated in free space so that three corners of the sample are set at  $z=0$  plane. Second, the best fit plane of the warped substrate is identified and the substrate is rotated so that the best fit plane is set at  $z=0$ . Fig. 4 shows (a) the initial fringe pattern image of a BGA substrate, (b) the 3D surface plot of the deformed BGA without position normalization, (c) the 3D surface plot with three-corner rotation to  $Z=0$ , and (d) the 3D surface plot rotated so that the best-fit-plane is set to  $Z=0$ .



(a)



(b)

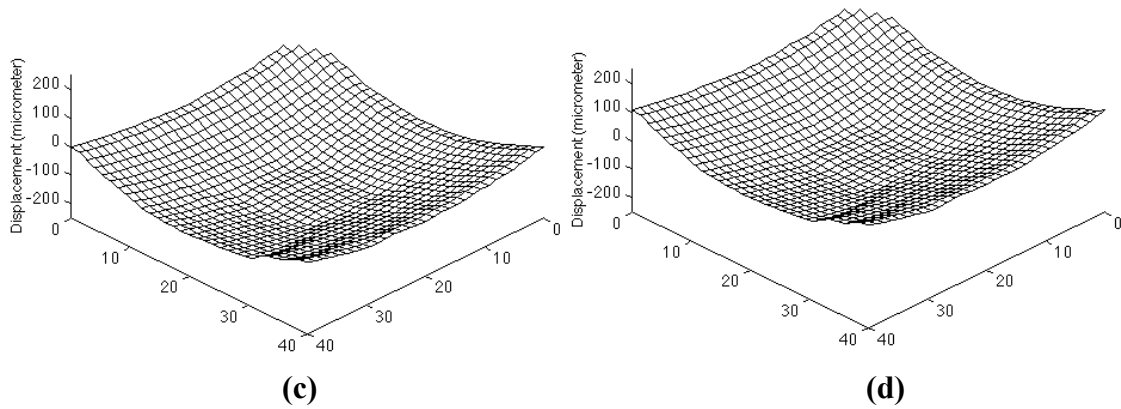


**Fig.4 Normalization of the Sample Position, (a) Initial Fringe Pattern, (b) Surface Plot without Rotation, (c) Surface Plot with Three-Corner Rotation and (d) Surface Plot with Best-Fit-Plane Rotation.**

### Measurement of BGA and PWB Interconnect Area Using Phase-Stepping

Fig. 5 shows the experimental set-up that is used for the measurement of the thermal deformation of BGAs and printed circuit boards. The system, commercially named *TherMoiré*<sup>®</sup>, was developed at the Advanced Electronic Packaging Laboratory at the Georgia Institute of Technology (Atlanta, Georgia USA)<sup>10</sup>. This system is capable of simulating a variety of soldering process, such as wave soldering and infrared reflow soldering. The testing sample is set inside of an isolated chamber. The grating is set on a stage that is driven by a computer controlled stepper motor. The temperature of the tested sample is measured by multiple thermocouples interfaced through signal conditioning circuitry to a desktop computer. The signal of a master thermocouple is compared with a user-entered temperature profile and the heater is then driven following the designated profile. Fringe pattern images are recorded in real-time by a CCD camera.

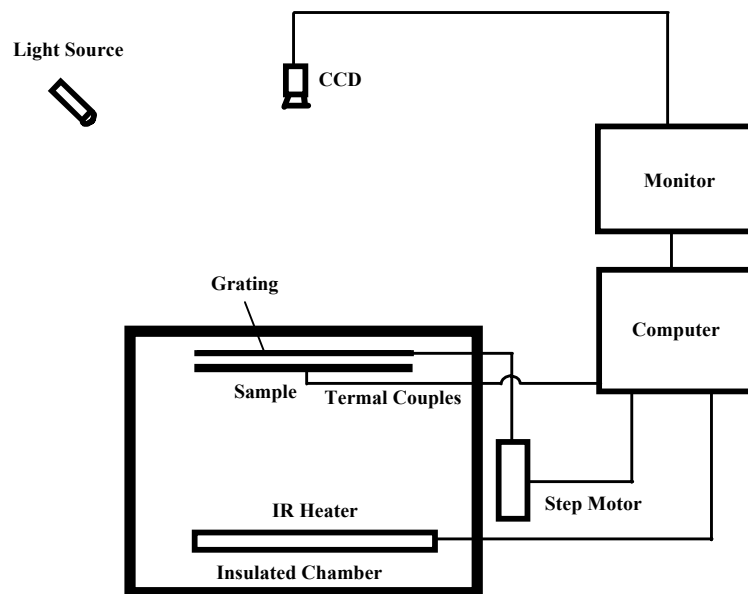


**Fig. 5 Set-up for the Measurement of Thermal Warpage of BGAs.**

A BGA (38×38mm) and its seating printed wiring board (PWB) were tested through a simulated reflow cycle. For the PWB, the phase-stepped measurement was made only on the interconnect area where the BGA was to be seated. The BGA sample was heated inside of the insulated chamber and the fringe pattern images were recorded at different temperature points. All data from the BGA was taken on the solder-ball side of the component. Solder-balls were removed in order to provide a planar, continuous surface. Each part was tested separately. The system configuration was such that the sensitivity was 8.47  $\mu\text{m}$  (3.33 mils) per fringe. At the peak temperature, 225 °C, the PWB was warped in a concave shape, while the BGA substrate was warped in a convex manner. The maximum gap between the two interconnect surfaces was as great as 428  $\mu\text{m}$ .

Fig. 6 plots the deformed BGA substrate and the PWB interconnect area at the peak temperature. The sample position has been normalized to a best-fit-plane and then the BGA has been moved up along the z-axis so that there is no overlap between the BGA and the PWB. Fig. 6 (b) shows the plot of the deformed samples along one diagonal (from top-left to bottom-right corners). The maximum gap is the difference of the maximum z value of the BGA and the minimum z value of PWB after the BGA has been translated along the z axis. Such a large gap between the BGA and its seating PWB due to their thermal warpage is very likely create problem during soldering process.

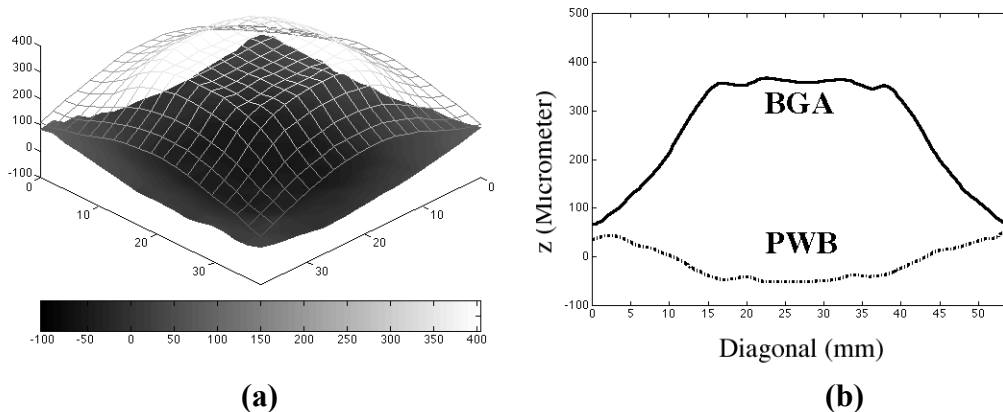


**Fig. 6 Thermal Warpage of BGA and its Seating PWB. (a) 3-D Surface Plot of the Deformed BGA and PWB at Peak Temperature 225 °C. (b) Deformation along the Diagonal of the BGA and the Seating Site of the PWB.**

## Conclusion

The analysis sensitivity of shadow moiré fringes pattern images is increased significantly when phase-stepping technique is applied. Phase-stepping technique makes use of the gray level information contained in the fringe pattern images so that the fractional fringe order may be resolved. The technique divides the gray level of the light intensity into 256 degrees. It can, theoretically speaking, resolve the fractional fringe to

1/256. In practice, a resolution of 0.1-0.01 fringe order is widely accepted. The ordering of fringes and the resulting generation of a displacement matrix for analysis is fully automated. Since the technique increased analysis sensitivity, the shadow moiré system remains environmentally insensitive. Thermal warpage of BGAs and electronic substrates can be successfully measured in real-time by the techniques and the system described in the paper. The application of the phase-stepping technique adds more powerful features to the existing shadow moiré system.

## Acknowledgment

The authors would like to express their thanks to EPS's customers who provided samples for testing, and Mr. Sean McCarron's help on the testing of the BGA and its seating PWB.

## References

1. F.P. Chiang, "Manual on Experimental Stress Analysis," J.F. Doyle and J.W. Phillips, Eds., SEM, Connecticut, Chapter 6, pp.107-135, 1989.
2. Y. Wang and P. Hassell, "Measurement of Thermal Deformation of BGA Using Phase-shifting Shadow Moiré," submitted to *Post Conference Proceedings, SEM 97' Spring Conference*, Bellevue, WA, June 2-4, 1997.
3. W.W. Macy, Jr., "Two-dimensional Fringe-pattern Analysis," *Applied Optics*, Vol.22, No.23, p3898-3901, 1983
4. C.A. Lee, T.G. Richards and R.E. Rowlands, "Exact Interpretation of Moiré Fringe Patterns in Digital Images," *Experimental Mechanics*, Vol.28, p409-416, 1988.
5. C.J. Morgan, "Least-Squares Estimation in Phase-Measurement Interferometry," *Optics Letters*, Vol.7, No.8, p368-370, 1982.
6. K. Creath, "Phase-Shifting Holographic Interferometry," Chap. 5, *Holographic Interferometry*, P.K. Rastogi Ed. Springer-Verlag, New York, 1994.
7. K. Creath, "Phase-Measurement Interferometry Techniques," Chap. 5, *Progress in Optics*, Vol.26, Elsevier Science Publishers B.V., 1988.
8. M. Chang and C. S. Ho, "Phase-measuring Profilometry Using Sinusoidal Grating," *Experimental Mechanics*, Vol.33, p117, 1993.
9. M. Chang, C.P. Hu, P. Lam and J.C. Wyant, "High Precision Deformation Measurement by Digital Phase Shifting Holographic Interferometry," *Applied Optics*, Vol.24, p3780, 1985.
10. M. Stiteler and C. Ume, "System for Real-Time Measurements of Thermally Induced Warpage in a Simulated Infrared Soldering Environment," *ASME Journal of Electronic Packaging*, Vol. 119, p1-7, 1997.
11. J.L. Sullivan, "Phase Stepped Fraction Moiré," *Experimental Mechanics*, Vol.31, p373, 1991.
12. K. Creath, "Phase-Measurement Interferometry Techniques," Chap. 5, *Progress in Optics*, Vol.26, Elsevier Science Publishers B.V., 1988.
13. D. Post, B. Han and P. Ifju, *High Sensitivity Moiré*, Springer-Verlag, New York, 1994.

14. G. Lai and T. Yatagai, "Generalized Phase-Shifting Interferometry," *J. Opt. Soc. Am. A*, Vol.8, No.5, p822-827, 1991.
15. Y.Y. Cheng and J.C. Wyant, "Phase Shifter Calibration in Phase-shifting Interferometry", *Applied Optics*, Vol.24, No.18, p3049, 1985.